Innsbruck Teleportation Experiment in the Wigner Formalism: A Realistic Description Based on the Role of the Zero-Point Field

Alberto Casado[1]*, Santiago Guerra[2] and José Plácido[2]

[1]Departamento de Física Aplicada III, Escuela Técnica Superior de Ingeniería, Universidad de Sevilla, Sevilla, Spain, [2]Grupo de Ingeniería Térmica e Instrumentación, Universidad de Las Palmas de Gran Canaria, Las Palmas de Gran Canaria, Spain

In this article, an undulatory description of the Innsbruck teleportation experiment is given, grounded in the role of the zero-point field (ZPF). The Wigner approach in the Heisenberg picture is used, so that the quadruple correlations of the field, along with the subtraction of the zero-point intensity at the detectors, are shown to be the essential ingredients that replace entanglement and collapse. This study contrasts sharply with the standard particle-like analysis and offers the possibility of understanding the hidden mechanism of teleportation, relying on vacuum amplitudes as hidden variables.

Keywords: teleportation, parametric downconversion, Wigner representation, local realism, zero-point field, Bell state measurement

1 INTRODUCTION

Since Bennett et al. proposed teleportation in 1993 [1], quantum state transmission has become essential for developing quantum computing and quantum communication [2, 3]. The standard theoretical approach to teleportation is based on the peculiar properties of Einstein–Podolsky–Rosen (EPR) pairs [4] in the Hilbert space. Entanglement and the projection postulate, along with the classical communication between the sender and receiver, often called Alice and Bob, respectively, constitute the fundamental elements of the teleportation protocol.

In the late 1990s, teleportation was achieved in experiments performed by the Universities of Innsbruck [5] and Rome [6], by using entangled photons generated in parametric downconversion (PDC). There is a discrepancy regarding who first performed genuine quantum teleportation [7]. On the one hand, the Innsbruck experiment used two pairs of entangled photons, and one of the four photons was used as a trigger to generate the single-particle state to be teleported [5, 8]. A remarkable characteristic of the four-photon source is the first experimental implementation of entanglement swapping [9, 10]. Nevertheless, given that the four polarization Bell states of two photons were not distinguishable using entanglement only in one degree of freedom and linear optics [11], the teleportation protocol described in Ref. 1 cannot be accomplished with 100% success in the Innsbruck scheme. Moreover, a controversial aspect of this experiment was the postselective or nonpostselective nature of teleportation [12–14]. On the other hand, in the Rome teleportation experiment, a pair of downconverted photons was used, and the state to be teleported was encoded in one of two degrees of freedom of one photon [15], which made a difference with respect to the work in Ref. 1. In contrast, the Bell state measurement (BSM) was accomplished with 100% success. In Ref. 16, a different implementation of the theoretical proposal given in Ref. 15 was carried out.

The Wigner formalism constitutes a complementary approach to the orthodox formulation in the Hilbert space for the study of quantum optical experiments implemented with PDC [17–25]. The

Wigner function of PDC is positive and allows for an intuitive picture in terms of stochastic processes. In the Wigner representation within the Heisenberg picture (WRHP), the dynamics is contained in the electric field and the Wigner distribution is time-independent, corresponding to the Wigner function of the vacuum state. In this approach, the linearity of the field equations of motion in the setup PDC plus linear optics can be exploited, to achieve relevant conclusions about quantum versus classical electrodynamics, by looking directly at the fields and their correlation properties. Recently, a more formal foundation of PDC has been developed using the Weyl–Wigner formalism [26].

One of the most interesting features of the WRHP approach is that the zero-point field (ZPF) appears in a natural form, which contributes to it being considered as a real stochastic field [27, 28]. The role of ZPF at the nonlinear crystal and idle channels of the optical devices placed between the source and detectors should be analyzed for a deeper understanding of the underlying physics. In this picture, photon entanglement can be understood as an interplay of correlated modes through the contribution of ZPF amplitudes in the polarization components of the field. Moreover, collapse is related to the subtraction of the zero-point intensity at the detectors, so that this approach clearly emphasizes the wave nature of light. The fact that detectors have a threshold gives rise to all nonclassical features of entangled photon pairs generated by PDC.

The standard analysis of a PDC experiment with the WRHP approach consists of the following steps:

i. Expression of the electric field amplitude corresponding to narrow light beams outgoing the nonlinear source is calculated. These beams are a linear transformation of the ZPF entering the crystal [17–19].

ii. Propagation of these fields throughout the experimental setup is conducted, following the rules of classical optics. At this step, the zero-point beams entering the idle channels of the optical devices must be considered.

iii. Calculation of the detection rates constitutes the main difference with respect to classical physics. In the case of single counts, the zero-point intensity is the threshold for detection, but the subtraction is more involved in the case of joint and multiple detection rates.

iv. The detection rates are expressed in terms of the field correlations mediated by the ZPF, allowing for a picture in terms of stochastic processes.

v. New physical insights emerge through the analysis of the different zero-point inputs. The role of the amplitude and phase of the fields in the light intensity at the detectors becomes relevant to the description of an internal mechanism leading to the different results. This analysis cannot be conducted with the standard treatment in the Hilbert space.

The combination of the possibility of transmitting and storing quantum information via the ZPF has revealed that the WRHP formalism is a very useful tool in analyzing the influence of the vacuum field in experiments on optical quantum communication

[29–34]. Specifically, this approach has been applied to the analysis of teleportation experiments, such as entanglement swapping [32] and the Rome teleportation experiment [33]. The study of the Rome experiment showed the great importance of the zero-point inputs in BSM [31], in such a way that the distinguishability of the four polarization-momentum Bell states of a single photon can be understood from a sufficient balance between the zero-point inputs at the source of entanglement and those that intervening in the Bell state analyzer. More recently, the role of the zero-point amplitudes as hidden variables on Bell state distinguishability and their application to teleportation [16] have been investigated [34].

In this article, a new picture of the Innsbruck teleportation experiment [5] is given, by using the WRHP approach. The importance of this proposal lies in understanding the physical properties of ZPF inputs that intervene in the experiment and emphasizing the wave nature of light and causal propagation of the fields involved. The article is organized as follows. In **Section 2**, the Wigner formalism in the Heisenberg framework is briefly reviewed. In **Section 3**, a general setup, including the one given in Ref. 5, is analyzed to investigate the relationship between teleportation and quadruple correlations. In **Section 4**, the relationship between different ZPF inputs at the setup and optimality of the BSM at Alice's station is analyzed. **Section 5** is devoted to the calculation of the fourfold detection probabilities in the Innsbruck experiment. Finally, in **Section 6**, the main conclusions of this work are presented along with further steps of this research line.

2 THE WIGNER REPRESENTATION WITHIN THE HEISENBERG PICTURE APPROACH FOR PARAMETRIC DOWNCONVERSION EXPERIMENTS

In this section, the mathematical tools used in the development of this work are described [17–19]. The field radiated by a nonlinear crystal is produced from the coupling between the ZPF and a classical wave representing the laser pumping beam. The vacuum is represented as a sum of two mutually complex conjugate amplitudes as follows:

$$\mathbf{E}_{\nu}\left(\mathbf{r}, t\right) = \mathbf{E}_{\nu}^{(+)}\left(\mathbf{r}, t\right) + \mathbf{E}_{\nu}^{(-)}\left(\mathbf{r}, t\right), \tag{1}$$

with

$$\mathbf{E}_{\nu}^{(+)}\left(\mathbf{r}, t\right) = i \sum_{\mathbf{k}, \lambda} \left(\frac{\hbar \omega_{\mathbf{k}}}{2L^3}\right)^{1/2} \alpha_{\mathbf{k}, \lambda} \mathbf{u}_{\mathbf{k}, \lambda} e^{i(\mathbf{k} \cdot \mathbf{r} - \omega_{\mathbf{k}} t)}, \tag{2}$$

$$\mathbf{E}_{\nu}^{(-)}\left(\mathbf{r}, t\right) = -i \sum_{\mathbf{k}, \lambda} \left(\frac{\hbar \omega_{\mathbf{k}}}{2L^3}\right)^{1/2} \alpha_{\mathbf{k}, \lambda}^{\star} \mathbf{u}_{\mathbf{k}, \lambda} e^{-i(\mathbf{k} \cdot \mathbf{r} - \omega_{\mathbf{k}} t)}. \tag{3}$$

The subscripted letter "ν" denotes the vacuum field or ZPF. L^3 is the normalization volume, $\alpha_{\mathbf{k}, \lambda}(t)$ is the amplitude corresponding to a mode whose wave vector is $\mathbf{k}$ and polarization vector is $\mathbf{u}_{\mathbf{k}, \lambda}$, with $\omega_{\mathbf{k}} = c|\mathbf{k}|$, and λ takes values in the set $\{H, V\}$, where $H(V)$ means horizontal (vertical).

Stochastic variables $\alpha^*_{\mathbf{k},\lambda}$ and $\alpha_{\mathbf{k},\lambda}$ follow a distribution given by the following Gaussian equation:

$$W(\alpha) = \prod_{\mathbf{k},\lambda} \frac{2}{\pi} e^{-2|\alpha_{\mathbf{k},\lambda}|^2} ; \alpha \equiv \{\alpha_{\mathbf{k},\lambda}\}. \tag{4}$$

On the other hand, the beam corresponding to the laser is represented by a plane wave with wave vector $\mathbf{k}_p$ and frequency ω_p. We have the following:

$$\mathbf{V}(\mathbf{r}, t) = \left(V_p(t) \exp\left[i\left(\mathbf{k}_p \cdot \mathbf{r} - \omega_p t\right)\right] + c.c. \right)\mathbf{u}; \mathbf{u} \perp \mathbf{k}_p, \tag{5}$$

where c.c. denotes complex conjugation. Given that the coherence time of the laser beam is usually large compared to most of the times involved, the amplitude $V_p(t)$ will be considered as a constant.

The electric field corresponding to a (narrow) light beam emitted by a nonlinear crystal is represented by the following slowly varying amplitude:

$$\mathbf{F}^{(+)}(\mathbf{r}, t) = ie^{\omega_s t} \sum_{\mathbf{k} \in [\mathbf{k}]_s, \lambda} \left(\frac{\hbar \omega_{\mathbf{k}}}{2L^3}\right)^{1/2} \alpha_{\mathbf{k},\lambda}(0)\mathbf{u}_{\mathbf{k},\lambda} e^{i(\mathbf{k}\cdot\mathbf{r} - \omega_{\mathbf{k}}t)}, \tag{6}$$

where ω_s represents the central frequency of the beam and $[\mathbf{k}]_s$ constitutes a set of wave vectors centered at $\mathbf{k}_s$. Amplitude $\alpha_{\mathbf{k},\lambda}(t = 0)$ has been calculated elsewhere to second order in a characteristic coupling constant (g) [17–19]. Type II PDC contains amplitudes $\alpha_{\mathbf{k},\lambda}$ $(\mathbf{k} \in [\mathbf{k}]_s)$, belonging to the zero-point beam entering the crystal in the direction of the signal, and the amplitudes $\alpha_{\mathbf{k}',\lambda'}$ $(\mathbf{k}' \in [\mathbf{k}]_i; \lambda' \neq \lambda)$, concerning the zero-point beam corresponding to the so-called idler photon, fulfilling the matching conditions $\omega_{\mathbf{k}} + \omega_{\mathbf{k}'} \approx \omega_p$ and $\mathbf{k} + \mathbf{k}' \approx \mathbf{k}_p$. For $t > 0$, there is a free evolution. The concrete expression of the fields exiting the crystal and the description of entanglement in the WRHP approach are reviewed in the next section.

Field amplitude $\mathbf{F}^{(+)}$ propagates through free space according to the following expression:

$$\mathbf{F}^{(+)}(\mathbf{r}_2, t) = \mathbf{F}^{(+)}\left(\mathbf{r}_1, t - \frac{r_{12}}{c}\right) e^{i\omega_s(r_{12}/c)} ; \mathbf{r}_{12} = |\mathbf{r}_2 - \mathbf{r}_1|. \tag{7}$$

Let us now review the theory of photodetection. The single detection probability at a given detector D_a is as follows:

$$P_a(\mathbf{r}, t) = K_a\langle I_a(\mathbf{r}, t) - I_{\nu,a}(\mathbf{r})\rangle, \tag{8}$$

where $\langle \ldots \rangle$ represents an average with the Wigner density given in **Eq. 4**. $I_a \propto \mathbf{E}_a^{(+)} \cdot \mathbf{E}_a^{(-)} = \mathbf{F}_a^{(+)} \cdot \mathbf{F}_a^{(-)}$, in appropriate units, is the intensity of light arriving at the detector and $I_{\nu,a}$ corresponds to the average intensity of the ZPF. On the other hand, K_a is a constant related to the effective efficiency of the detection process at detector D_a.

In experiments involving polarization, the joint detection probability is calculated by using the following expression:

$$P_{ab}(\mathbf{r}, t; \mathbf{r}', t') = K_a K_b \times \sum_{\lambda,\lambda'} \left|\langle F_{a,\lambda}^{(+)}(\phi_a; \mathbf{r}, t) F_{b,\lambda'}^{(+)}(\phi_b; \mathbf{r}', t')\rangle\right|^2, \tag{9}$$

where ϕ_A and ϕ_B, appearing in the cross-correlation $\langle F_{a,\lambda}^{(+)} F_{b,\lambda'}^{(+)}\rangle$, represent setup parameters. In the situation where the operators

corresponding to fields in detectors D_a and D_b commute, as in the case of Bell-type experiments [35], the previous expression is equivalent to the average of product $K_a K_b(I_a - I_{\nu,a})(I_b - I_{\nu,b})$. Nevertheless, in a general situation, the subtraction of the pure zero-point contribution is more involved.

Finally, in experiments involving fourfold detection, the detection probability can be obtained as the sum of sixteen addends. We have the following:

$$P_{abcd}(\mathbf{r}, t; \mathbf{r}', t'; \mathbf{r}'', t''; \mathbf{r}''', t''') = K_a K_b K_c K_d$$
$$\times \sum_{\lambda,\lambda',\lambda'',\lambda'''} \left|\langle F_{a,\lambda}^{(+)}(\phi_a; \mathbf{r}, t) F_{b,\lambda'}^{(+)}(\phi_b; \mathbf{r}', t') F_{c,\lambda''}^{(+)}(\phi_c; \mathbf{r}'', t'') F_{d,\lambda'''}^{(+)}(\phi_d; \mathbf{r}''', t''')\rangle\right|^2, \tag{10}$$

where the quadruple correlation $\langle F_{a,\lambda}^{(+)} F_{b,\lambda'}^{(+)} F_{c,\lambda''}^{(+)} F_{d,\lambda'''}^{(+)}\rangle$ can be calculated in terms of the cross-correlation properties of the fields, by taking into account the fact that the field amplitudes in PDC are Gaussian. That is,

$$\langle F_{a,\lambda}^{(+)} F_{b,\lambda'}^{(+)} F_{c,\lambda''}^{(+)} F_{d,\lambda'''}^{(+)}\rangle = \langle F_{a,\lambda}^{(+)} F_{b,\lambda'}^{(-)}\rangle\langle F_{c,\lambda''}^{(-)} F_{d,\lambda'''}^{(+)}\rangle + \langle F_{a,\lambda}^{(+)} F_{c,\lambda''}^{(+)}\rangle$$
$$\times \langle F_{b,\lambda'}^{(+)} F_{d,\lambda'''}^{(+)}\rangle + \langle F_{a,\lambda}^{(+)} F_{d,\lambda'''}^{(+)}\rangle\langle F_{b,\lambda'}^{(+)} F_{c,\lambda''}^{(+)}\rangle. \tag{11}$$

In actual experiments, **Eqs 8–10** must be integrated over the surface aperture of the detectors and appropriate detection windows.

3 THE MEANING OF TELEPORTATION IN TERMS OF THE QUADRUPLE CORRELATIONS

The standard description of teleportation in the Hilbert space [1] uses three particles, one of them (particle 1) in an unknown quantum state to be teleported, $|\phi\rangle_1 = \alpha|H\rangle_1 + \beta|V\rangle_1$, and two entangled particles (particles 2 and 3) in a singlet state, $|\psi^-\rangle_{23}$. The state of the three-particle system is given by the tensor product:

$$|\psi\rangle_{123} = |\phi\rangle_1 |\psi^-\rangle_{23}$$
$$= -\frac{1}{2}|\psi^-\rangle_{12}\left(\alpha|H\rangle_3 + \beta|V\rangle_3\right) - \frac{1}{2}|\psi^+\rangle_{12}\left(\alpha|H\rangle_3 - \beta|V\rangle_3\right)$$
$$+ \frac{1}{2}|\phi^-\rangle_{12}\left(\beta|H\rangle_3 + \alpha|V\rangle_3\right) + \frac{1}{2}|\phi^+\rangle_{12}\left(\beta|H\rangle_3 - \alpha|V\rangle_3\right), \tag{12}$$

where the four Bell-base states are

$$|\psi^\pm\rangle_{ij} = \frac{1}{\sqrt{2}}\left[|H\rangle_i|V\rangle_j \pm |V\rangle_i|H\rangle_j\right], \tag{13}$$

$$|\phi^\pm\rangle_{ij} = \frac{1}{\sqrt{2}}\left[|H\rangle_i|H\rangle_j \pm |V\rangle_i|V\rangle_j\right]. \tag{14}$$

A BSM on particles 1 and 2 leaves particle 3 in a state that can be modified after classical communication, to reproduce the initial state of particle 1. If the BSM indicates the detection of a singlet state of particles 1 and 2, then teleportation is directly achieved.
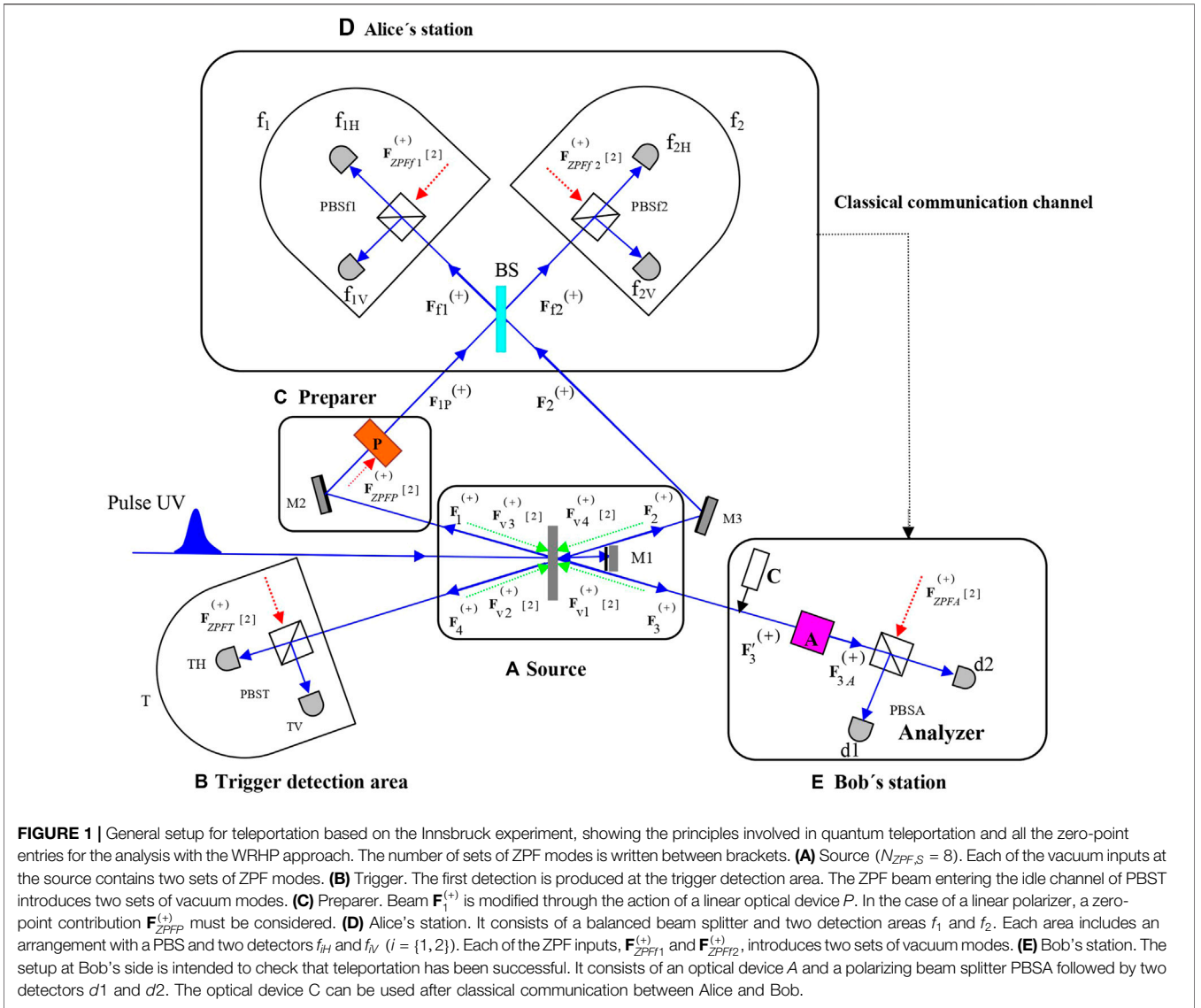
FIGURE 1 | General setup for teleportation based on the Innsbruck experiment, showing the principles involved in quantum teleportation and all the zero-point entries for the analysis with the WRHP approach. The number of sets of ZPF modes is written between brackets. **(A)** Source ($N_{ZPF,S} = 8$). Each of the vacuum inputs at the source contains two sets of ZPF modes. **(B)** Trigger. The first detection is produced at the trigger detection area. The ZPF beam entering the idle channel of PBST introduces two sets of vacuum modes. **(C)** Preparer. Beam $\mathbf{F}_1^{(+)}$ is modified through the action of a linear optical device P. In the case of a linear polarizer, a zero-point contribution $\mathbf{F}_{ZPFP}^{(+)}$ must be considered. **(D)** Alice's station. It consists of a balanced beam splitter and two detection areas f_1 and f_2. Each area includes an arrangement with a PBS and two detectors f_{iH} and f_{iV} ($i = \{1,2\}$). Each of the ZPF inputs, $\mathbf{F}_{ZPF1}^{(+)}$ and $\mathbf{F}_{ZPF2}^{(+)}$, introduces two sets of vacuum modes. **(E)** Bob's station. The setup at Bob's side is intended to check that teleportation has been successful. It consists of an optical device A and a polarizing beam splitter PBSA followed by two detectors $d1$ and $d2$. The optical device C can be used after classical communication between Alice and Bob.

In the Innsbruck experiment, two independent pairs of downconverted photons are "simultaneously" produced in the state $|\Pi\rangle_{1234} = |\psi^-\rangle_{14} |\psi^-\rangle_{23}$. Photon 4 is used as a trigger to generate the state described in **Eq. 12**, once a given transformation is applied on photon 1.

In the WRHP approach, a deep understanding of this experiment requires the analysis of the quadruple correlation properties of the field. Let us consider the sketch of the experimental setup described in **Figure 1**. The notation used in this figure is similar to the one given in Ref. 5, with the goal of an easier reading of this article and the possibility of comparing it with the original setup. In addition, ZPF inputs are represented for understanding the original ideas displayed in this work and its relationship with the standard description in the Hilbert space formulation. Four two-by-two correlated beams represent two couples of polarization-entangled photons. The input fields $\mathbf{F}_{v1}^{(+)}$ and $\mathbf{F}_{v4}^{(+)}$ ($\mathbf{F}_{v2}^{(+)}$ and $\mathbf{F}_{v3}^{(+)}$), each containing two sets of vacuum modes, are coupled with the laser, giving rise to the correlated

signals $\mathbf{F}_1^{(+)}$ and $\mathbf{F}_4^{(+)}$ ($\mathbf{F}_2^{(+)}$ and $\mathbf{F}_3^{(+)}$). The quantum information is carried out by eight sets of ZPF modes that are amplified at the source, that is,

$$N_{ZPF,S} = 8. \tag{15}$$

The exiting fields at the center of the nonlinear source can be expressed to second order in the coupling parameter using the following amplitudes (for simplicity, space-time notation is discarded):

$$F_1^{(+)} = \begin{bmatrix} F_s^{(+)} \\ F_p^{(+)} \end{bmatrix} = \begin{bmatrix} (1 + g^2|V|^2J)F_{v1,H}^{(+)} + gVGF_{v4,V}^{(-)} \\ (1 + g^2|V|^2J)F_{v1,V}^{(+)} + gVGF_{v4,H}^{(-)} \end{bmatrix}, \tag{16}$$

$$F_4^{(+)} = \begin{bmatrix} F_q^{(+)} \\ e^{i\pi}F_r^{(+)} \end{bmatrix} = \begin{bmatrix} (1 + g^2|V|^2J)F_{v4,H}^{(+)} + gVGF_{v1,V}^{(-)} \\ e^{i\pi}\left[(1 + g^2|V|^2J)F_{v4,V}^{(+)} + gVGF_{v1,H}^{(-)} \right] \end{bmatrix}, \tag{17}$$

$$F_2^{(+)} = \begin{bmatrix} F_s'^{(+)} \\ F_p'^{(+)} \end{bmatrix} = \begin{bmatrix} (1 + g^2|V|^2J)F_{v2,H}^{(+)} + gV'GF_{v3,V}^{(-)} \\ (1 + g^2|V|^2J)F_{v2,V}^{(+)} + gV'GF_{v3,H}^{(-)} \end{bmatrix}, \tag{18}$$

$$F_3^{(+)} = \begin{bmatrix} F'_q^{(+)} \\ e^{i\pi}F'_r^{(+)} \end{bmatrix} = \begin{bmatrix} \left(1 + g^2|V|^2 J\right)F_{v3,H}^{(+)} + gV'GF_{v2,V}^{(-)} \\ e^{i\pi}\left[\left(1 + g^2|V|^2 J\right)F_{v3,V}^{(+)} + gV'GF_{v2,H}^{(-)}\right] \end{bmatrix},$$

(19)

where G and J are linear operators defined elsewhere [17–19] and are related to the selection of modes fulfilling the matching conditions. On the other hand, $V' = -V$ due to the reflection of the pumping beam at mirror M1. It will be considered that M1 is in a fixed position, such that the condition of temporal overlap at the beam splitter is fulfilled [5].

Equations 16–19 correspond to the WRHP description of the state vector $|\Pi\rangle_{1234} = |\Psi^-\rangle_{14}|\Psi^-\rangle_{23}$, the crucial point being the interplay of correlated fields, through the action of the zero-point amplitudes: the only nonnull cross-correlations are those concerning the labels (p,q) and (r,s) of beams 1–4 and the same for the beams 2–3. This can be easily understood by taking into account the fact that $F_{vj,X}^{(+)}$ ($j = \{1,2,3,4\}$, $X = \{H,V\}$) is only correlated with $F_{vj,X}^{(-)}$, being a direct consequence of **Eq. 4**. Any of the four cross-correlations can be expressed, at any position and time, in terms of the corresponding one at the center of the nonlinear source (see **Eq. 7**). We have the following:

$$\langle F_p^{(+)}(0,t)F_q^{(+)}(0,t')\rangle = \langle F_r^{(+)}(0,t)F_s^{(+)}(0,t')\rangle = gV\nu(t-t'),$$

(20)

where $\nu(t-t')$ is a function that vanishes when $|t-t'| > \tau$, t being the correlation time between the downconverted photons. Similar relations hold for the corresponding primed amplitudes. In addition, the exponential factor ($e^{i\pi}$) in **Eqs 17** and **19** gives rise to a sign difference between the two correlations, corresponding to orthogonal polarization amplitudes, involving the couple of beams $1 - 4$ ($2-3$). This sign difference identifies the physical properties of the singlet state in the WRHP formalism [29, 30].

Moreover, the amplitude $\mathbf{F}_p^{(+)}$ verifies the following autocorrelation property:

$$\langle F_p^{(+)}(0,t)F_p^{(-)}(0,t')\rangle - \langle F_{v1,V}^{(+)}(0,t)F_{v1,V}^{(-)}(0,t')\rangle = g^2|V|^2\mu(t-t'),$$

(21)

where $\mu(t-t')$ is a function that goes to zero when $|t-t'| > \tau$. Similar relations hold for the rest of the field amplitudes given in **Eqs 16–19**.

By taking into account **Eq. 20**, the two nonnull cross-correlations concerning beams 1 and 4 can be expressed in the following compact form:

$$\langle F_{4,X}^{(+)}(0,t)F_{1,U}^{(+)}(0,t')\rangle = (-1)^{n(X)}gV\nu(t-t')[1-\delta_{XU}], \quad (22)$$

where X and U can take values in the set $\{H,V\}$. On the other hand, $n(H) = 2$ and $n(V) = 1$. A similar expression holds for the correlations involving beams 2 and 3, that is,

$$\langle F_{2,X}^{(+)}(0,t)F_{3,U}^{(+)}(0,t')\rangle = (-1)^{n(X)+1}gV'\nu(t-t')[1-\delta_{XU}]. \quad (23)$$

The quadruple correlations representing the fields given in **Eqs 16–19** can be calculated using **Eq. 11**. Given that beam 1 (2) is only correlated with 4 (3), there are four nonnull correlations:

$$\langle F_{4,X}^{(+)}(0,t)F_{1,U}^{(+)}(0,t')F_{2,W}^{(+)}(0,t'')F_{3,Z}^{(+)}(0,t''')\rangle$$
$$= (-1)^{n(X)+n(W)+1}g^2 VV'\nu(t-t')\nu(t''-t''')[1-\delta_{XU}][1-\delta_{WZ}],$$

(24)

where X, U, Z, and W can take values in the set $\{H,V\}$.

From now on, for notation simplicity, an identical distance between the source and the different detectors will be considered, so that the phase shift in **Eq. 7** will not be considered in the expression of the fields. Moreover, for the time being, the dependence of the fields on position and time will be discarded. Nevertheless, the reader's attention can be drawn, wherever necessary, to any reintroduction of space-time variables.

In the Innsbruck experiment, the first detection is produced at the trigger detector. Let us suppose that the trigger detection area involves a polarizing beam splitter PBST that transmits (reflects) horizontal (vertical) polarization. Two detectors, TH and TV, are placed at each of the exiting channels. The fields at the detectors have a noise component coming from the ZPF entering the idle channel of PBST, that is,

$$F_{TH}^{(+)} = \begin{pmatrix} F_q^{(+)} \\ iF_{ZPFT,V}^{(+)} \end{pmatrix}; F_{TV}^{(+)} = \begin{pmatrix} F_{ZPFT,H}^{(+)} \\ -iF_r^{(+)} \end{pmatrix}. \quad (25)$$

Let us now consider the action of a linear optical device on beam 1. The transmitted field amplitude $\mathbf{F}_{1P}^{(+)}$ is

$$\mathbf{F}_{1P}^{(+)} = \widehat{P}\mathbf{F}_1^{(+)} = \begin{bmatrix} L_H & R_H \\ L_V & R_V \end{bmatrix}\begin{bmatrix} F_s^{(+)} \\ F_p^{(+)} \end{bmatrix} = \begin{bmatrix} L_H F_s^{(+)} + R_H F_p^{(+)} \\ L_V F_s^{(+)} + R_V F_p^{(+)} \end{bmatrix},$$

(26)

where P denotes the word "preparer" and L (R) is the left (right) column of $\widehat{P}$.

In the case of a circular polarizer of angle θ with respect to horizontal, $L_H = \cos^2\theta$, $R_H = L_V = \cos\theta\sin\theta$, and $R_V = \sin^2\theta$. In this situation, a zero-point contribution $\mathbf{F}_{ZPFP}^{(+)}$ must be added in **Eq. 26**. This ZPF amplitude is uncorrelated with the rest of the fields. Thus, $\mathbf{F}_{1P}^{(+)}$ can be generally expressed as follows:

$$\mathbf{F}_{1P}^{(+)} = \begin{bmatrix} P_H\left(F_s^{(+)}, F_p^{(+)}\right) \\ P_V\left(F_s^{(+)}, F_p^{(+)}\right) \end{bmatrix}, \quad (27)$$

where

$$P_H\left(F_s^{(+)}, F_p^{(+)}\right) = L_H F_s^{(+)} + R_H F_p^{(+)} + F_{ZPFP,H}^{(+)},$$
$$P_V\left(F_s^{(+)}, F_p^{(+)}\right) = L_V F_s^{(+)} + R_V F_p^{(+)} + F_{ZPFP,V}^{(+)}.$$

(28)

The general transformation given in **Eq. 28** represents a great variety of experiments with different preparations so that the analysis displayed in this article goes beyond the experimental situation given in Ref. 5, where a linear polarizer acts on beam $\mathbf{F}_1^{(+)}$. As a matter of fact, the previous analysis of entanglement swapping given in Ref. 32, where $\widehat{P} = \widehat{I}$, can be seen as a particular case of the results presented in this work.

Using **Eqs 17**, **20**, **27**, and **28**, we have the following four cross-correlations concerning beams $\mathbf{F}_{1P}^{(+)}$ and $\mathbf{F}_4^{(+)}$:

$$\langle F_{4,X}^{(+)}F_{1P,U}^{(+)}\rangle = (-1)^{n(X)}gV\nu(0)F(X,U), \quad (29)$$

where the bivariate function $F(X, U)$ is given by

$$F(X, U) = L_U \delta_{X,V} + R_U \delta_{X,H}. \tag{30}$$

This leads to a duplication of the nonnull quadruple correlations, from four to eight. Using **Eqs 11**, **23**, and **29**, we have the following:

$$\langle F_{4,X}^{(+)} F_{1P,U}^{(+)} F_{2,W}^{(+)} F_{3,Z}^{(+)} \rangle = \langle F_{4,X}^{(+)} F_{1P,U}^{(+)} \rangle \langle F_{2,W}^{(+)} F_{3,Z}^{(+)} \rangle$$
$$= (-1)^{n(X)+n(W)+1} g^2 VV' \nu^2(0) F(X, U) [1 - \delta_{WZ}]. \tag{31}$$

Let us now calculate the fields at Alice's station. Beams $\mathbf{F}_{1P}^{(+)}$ and $\mathbf{F}_2^{(+)}$ are superposed at a balanced beam splitter (see **Figure 1**) so that the number of sets of amplified modes entering the Bell state analyzer is as follows (see **Eq. 15**) [33]:

$$N_{ZPF,A} = \frac{N_{ZPF,S}}{2} = 4. \tag{32}$$

From **Eqs 18**, **27**, and **28**, the exiting beam ($\mathbf{F}_{fj}^{(+)} j = 1, 2$) is given by the following superposition:

$$\mathbf{F}_{fj}^{(+)} = -i^j \frac{(-1)^j \mathbf{F}_{1P}^{(+)} + i\mathbf{F}_2^{(+)}}{\sqrt{2}} = -\frac{i^j}{\sqrt{2}} \begin{bmatrix} (-1)^j P_H\left(F_s^{(+)}, F_p^{(+)}\right) + iF_s'^{(+)} \\ (-1)^j P_V\left(F_s^{(+)}, F_p^{(+)}\right) + iF_p'^{(+)} \end{bmatrix}. \tag{33}$$

Now, to get the electric field at the detector f_{jX} ($X = \{H, V\}$), a ZPF component coming from the idle channel of PBSfj must be included. That is,

$$\mathbf{F}_{fjH}^{(+)} = -\frac{i^j}{\sqrt{2}} \left[(-1)^j P_H\left(F_s^{(+)}, F_p^{(+)}\right) + iF_s'^{(+)} \right] + iF_{ZPFfj,V}^{(+)}, \tag{34}$$

$$\mathbf{F}_{fjV}^{(+)} = -\frac{i^{j+1}}{\sqrt{2}} \left[(-1)^j P_V\left(F_s^{(+)}, F_p^{(+)}\right) + iF_p'^{(+)} \right] + F_{ZPFfj,H}^{(+)}. \tag{35}$$

In the standard description of quantum teleportation [1], Alice informs Bob of her measurement result via a classical communication channel. In this way, Bob can apply a linear transformation on beam $\mathbf{F}_3^{(+)}$ by means of the optical device C (see **Figure 1**), to reproduce the prepared state. Then, in order to verify that teleportation has been successfully carried out, the signal $\mathbf{F}_3'^{(+)} = \widehat{C} F_3^{(+)}$ enters an analyzer consisting of a linear optical device A followed by a polarizing beam splitter, PBSA. Let $\mathbf{F}_{3A}^{(+)}$ be the signal entering PBSA, that is, $\mathbf{F}_{3A}^{(+)} = \widehat{A} \mathbf{F}_3'^{(+)} = \widehat{A}\widehat{C} F_3^{(+)}$; then, we have the following:

$$\mathbf{F}_{3A}^{(+)} = \begin{bmatrix} \tilde{L}_H & \tilde{R}_H \\ \tilde{L}_V & \tilde{R}_V \end{bmatrix} \begin{bmatrix} F_q'^{(+)} \\ -F_r'^{(+)} \end{bmatrix} = \begin{bmatrix} \tilde{A}_H\left(F_q'^{(+)}, F_r'^{(+)}\right) \\ \tilde{A}_V\left(F_q'^{(+)}, F_r'^{(+)}\right) \end{bmatrix}, \tag{36}$$

$$\tilde{A}_H\left(F_q'^{(+)}, F_r'^{(+)}\right) = \tilde{L}_H F_q'^{(+)} - \tilde{R}_H F_r'^{(+)}, \tag{37}$$

$$\tilde{A}_V\left(F_q'^{(+)}, F_r'^{(+)}\right) = \tilde{L}_V F_q'^{(+)} - \tilde{R}_V F_r'^{(+)}, \tag{38}$$

where the matrix $\widehat{A}\widehat{C}$ is represented by parameters $\tilde{L}_H$, $\tilde{L}_V$, $\tilde{R}_H$, and $\tilde{R}_V$. It has been considered that neither $\widehat{C}$ nor $\widehat{A}$ introduces additional ZPF modes.

Finally, by considering the ZPF entering the idle channel of PBSA, the field amplitudes at detectors d_1 and d_2 are given by

$$\mathbf{F}_{d_2}^{(+)} = \begin{bmatrix} \tilde{A}_H\left(F_q'^{(+)}, F_r'^{(+)}\right) \\ iF_{ZPF,AV}^{(+)} \end{bmatrix}; \mathbf{F}_{d_1}^{(+)} = \begin{bmatrix} F_{ZPF,AH}^{(+)} \\ i\tilde{A}_V\left(F_q'^{(+)}, F_r'^{(+)}\right) \end{bmatrix}. \tag{39}$$

From **Eqs 18**, **20**, **37**, and **38**, the following four cross-correlations, involving beams $F_2^{(+)}$ and $F_{3A}^{(+)}$, are obtained:

$$\langle F_{2,W}^{(+)} F_{3A,Z}^{(+)} \rangle = (-1)^{n(W)+1} gV' \nu(0) \tilde{F}(W, Z), \tag{40}$$

where

$$\tilde{F}(W, Z) = \tilde{L}_Z \delta_{W,V} + \tilde{R}_Z \delta_{W,H}. \tag{41}$$

3.1 Analysis of the Quadruple Correlations

The quadruple correlations play a fundamental role in the calculation of fourfold detection probabilities (see **Eq. 10**). Given that the zero-point beams entering the idle channels of the PBSs placed before the detectors are uncorrelated with the signals and with each other, the understanding of the Innsbruck experiment requires a detailed analysis of the correlation $\langle F_{4,X}^{(+)} F_{fj,U}^{(+)} F_{fk,W}^{(+)} F_{3A,Z}^{(+)} \rangle$ involving the fields given in **Eqs 17**, **33**, and **36**. Using **Eq. 11** and taking into consideration that beam 4 (3) is only correlated with 1 (2), the following expression is obtained:

$$\langle F_{4,X}^{(+)} F_{fj,U}^{(+)} F_{fk,W}^{(+)} F_{3A,Z}^{(+)} \rangle = \frac{1}{2} i^{j+k+1} (-1)^j \left[\langle F_{4,X}^{(+)} F_{1P,U}^{(+)} \rangle \langle F_{2,W}^{(+)} F_{3A,Z}^{(+)} \rangle + (-1)^{k-j} \langle F_{4,X}^{(+)} F_{1P,W}^{(+)} \rangle \langle F_{2,U}^{(+)} F_{3A,Z}^{(+)} \rangle \right]. \tag{42}$$

Now, substituting **Eqs 29** and **40** into **Eq. 42**, we get

$$\langle F_{4,X}^{(+)} F_{fj,U}^{(+)} F_{fk,W}^{(+)} F_{3A,Z}^{(+)} \rangle = \frac{1}{2} i^{j+k+1} (-1)^j g^2 VV' \nu^2(0) (-1)^{n(X)+n(W)+1}$$
$$\times \left[F(X, U) \tilde{F}(W, Z) + (-1)^{k-j} (-1)^{n(U)-n(W)} F(X, W) \tilde{F}(U, Z) \right]. \tag{43}$$

As will be demonstrated below, a detailed analysis of **Eqs 42** and **43** provides an understanding of physics behind teleportation without the necessity of collapse as a crucial ingredient. Let us divide this study into two parts: (i) the properties of the quadruple correlations in terms of the fields at Alice's station will provide a better understanding of the indistinguishability of the four Bell states given in **Eq. 12** [11, 32]; (ii) the analysis of quadruple correlations by looking at beams $\mathbf{F}_4^{(+)}$ and $\mathbf{F}_3^{(+)}$, that is, by putting $\widehat{A}\widehat{C} = \widehat{I}$, will offer a complete comprehension of the Innsbruck experiment in terms of correlated modes.

3.1.1 Quadruple Correlations and Bell State Measurement

Let us consider the following situations, according to the values of the polarizations U and W given in **Eq. 42**:

(a) First let us focus on the case of $U = W$. We have the following:

$$\langle F_{4,X}^{(+)}F_{fj,U}^{(+)}F_{fk,U}^{(+)}F_{3A,Z}^{(+)}\rangle = \frac{1}{2}i^{j+k+1}(-1)^j\langle F_{4,X}^{(+)}F_{1P,U}^{(+)}\rangle\langle F_{2,U}^{(+)}F_{3A,Z}^{(+)}\rangle\big[1+(-1)^{k-j}\big].$$
(44)

a.1. The above expression is equal to zero in the case of $j \neq k$, that is when the field amplitudes corresponding to the same polarization of different beams are considered. This result justifies that a double detection in detectors f_{1H} and f_{2H}, or in f_{1V} and f_{2V}, cannot be produced (see **Figure 1**).

a.2. In the case of $j = k$, **Eq. 44** leads to

$$\langle F_{4,X}^{(+)}F_{fj,U}^{(+)}F_{fj,U}^{(+)}F_{3A,Z}^{(+)}\rangle = i\langle F_{4,X}^{(+)}F_{1P,U}^{(+)}\rangle\langle F_{2,U}^{(+)}F_{3A,Z}^{(+)}\rangle.$$
(45)

This situation corresponds to a joint detection at any of the four detectors located in Alice's station and is related to the detection of one of the two indistinguishable states $|\phi^+\rangle_{12}$ or $|\phi^-\rangle_{12}$ [32].

b. Let us now analyze the $U \neq W$ situation; that is, the amplitudes at Alice's station have orthogonal polarization.

b.1. Let us first consider the case of j=k, where both polarizations of the same beam, namely, $F_{fj,H}^{(+)}$ and $F_{fj,V}^{(+)}$, are involved. From **Eq. 42**, we have the following:

$$\langle F_{4,X}^{(+)}F_{fj,U}^{(+)}F_{fj,W}^{(+)}F_{3A,Z}^{(+)}\rangle = \frac{i}{2}\big[\langle F_{4,X}^{(+)}F_{1P,U}^{(+)}\rangle\langle F_{2,W}^{(+)}F_{3A,Z}^{(+)}\rangle + \langle F_{4,X}^{(+)}F_{1P,W}^{(+)}\rangle$$
$$\times\langle F_{2,U}^{(+)}F_{3A,Z}^{(+)}\rangle\big].$$
(46)

From the above equation, the following symmetry property is derived:

$$\langle F_{4,X}^{(+)}F_{fj,U}^{(+)}F_{fj,W}^{(+)}F_{3A,Z}^{(+)}\rangle = \langle F_{4,X}^{(+)}F_{fj,W}^{(+)}F_{fj,U}^{(+)}F_{3A,Z}^{(+)}\rangle,$$
(47)

which implies that the correlation remains invariant under the exchange $U\leftrightarrow W$. This property is related to the detection of the state $|\psi^+\rangle_{12}$ when a joint detection is produced in f_{1H} and f_{1V} or in f_{2H} and f_{2V}.

b.2. Finally, the cases of $U \neq W$ and $j \neq k$ correspond to the situation in which the orthogonal polarization of different beams is involved. From **Eq. 42**, the corresponding quadruple correlation is

$$\langle F_{4,X}^{(+)}F_{fj,U}^{(+)}F_{fk,W}^{(+)}F_{3A,Z}^{(+)}\rangle = \frac{1}{2}(-1)^j\big[\langle F_{4,X}^{(+)}F_{1P,U}^{(+)}\rangle\langle F_{2,W}^{(+)}F_{3A,Z}^{(+)}\rangle$$
$$- \langle F_{4,X}^{(+)}F_{1P,W}^{(+)}\rangle\langle F_{2,U}^{(+)}F_{3A,Z}^{(+)}\rangle\big],$$
(48)

and the following antisymmetric property can be easily deduced:

$$\langle F_{4,X}^{(+)}F_{fj,U}^{(+)}F_{fk,W}^{(+)}F_{3A,Z}^{(+)}\rangle = -\langle F_{4,X}^{(+)}F_{fj,W}^{(+)}F_{fk,U}^{(+)}F_{3A,Z}^{(+)}\rangle.$$
(49)

This sign difference under the exchange $U\leftrightarrow W$ is related to the detection of the state $|\psi^-\rangle_{12}$ when a joint detection is produced at detectors f_{1H} and f_{2V}, or in f_{1V} and f_{2H}.

3.1.2 Quadruple Correlations and Teleportation

From now on, let us focus on the situation in which no transformation is applied on beam $\mathbf{F}_3^{(+)}$, that is, $\widehat{C} = \widehat{A} = \widehat{I}$, so that $\mathbf{F}_{3A}^{(+)} = \mathbf{F}_3^{(+)}$. In Ref. 32, it is demonstrated that, for $\widehat{P} = \widehat{I}$, a joint detection in f_{1H} and f_{2V} (f_{1V} and f_{2H}) leads to the transfer of the correlation properties that characterize the singlet state $|\Psi^-\rangle_{12}$ to the beams $\mathbf{F}_4^{(+)}$ and $\mathbf{F}_3^{(+)}$, mediated by the quadruple correlations of the field, even when $\mathbf{F}_4^{(+)}$ and $\mathbf{F}_3^{(+)}$ are uncorrelated (entanglement swapping in the WRHP approach). The key point in that analysis is the sign flip in the correlations involving orthogonal polarization components of beams $\mathbf{F}_4^{(+)}$ and $\mathbf{F}_3^{(+)}$, for $j \neq k$ and $U \neq W$, under the exchange $X\leftrightarrow Z$ (see equations (33)–(36) of Ref. 32).

Let us now address the action of a linear polarizer on beam $\mathbf{F}_1^{(+)}$, so that $\mathbf{F}_{1P}^{(+)}$ represents linearly polarized light. Given that the correlation properties corresponding to the beams exiting the crystal (see **Eqs 16–19**) are rotationally invariant [29], $\mathbf{F}_4^{(+)}$ behaves like a polarized beam with orthogonal polarization to the one corresponding to $\mathbf{F}_{1P}^{(+)}$, mediated by the cross-correlation properties given in **Eq. 29**. As demonstrated below, once detection is produced at the trigger area, a joint detection in f_{1H} (f_{1V}) and f_{2V} (f_{2H}) gives rise to the teleportation of the polarization properties from $\mathbf{F}_{1P}^{(+)}$ to $\mathbf{F}_3^{(+)}$.

To demonstrate teleportation in the WRHP approach, a sign flip is required under the exchange $X\leftrightarrow Z$ in **Eq. 48**, for $\widehat{C} = \widehat{A} = \widehat{I}$. In this case, $\tilde{L}_H = \tilde{R}_V = 1$ and $\tilde{R}_H = \tilde{L}_V = 0$, so that $\tilde{F}(U,W) = 1 - \delta_{UW}$ (see **Eq. 41**). In this situation, **Eq. 43**, for $j \neq k$ and $U \neq W$, leads to

$$\langle F_{4,X}^{(+)}F_{fj,U}^{(+)}F_{fk,W}^{(+)}F_{3,Z}^{(+)}\rangle = \frac{(-1)^j}{2}(-1)^{n(X)+n(W)+1}g^2VV'\nu^2(0)$$
$$\times [F(X,U)(1-\delta_{WZ})$$
$$+ F(X,W)(1-\delta_{UZ})].$$
(50)

Given that $U \neq W$, one of the two addends must be zero. Let us take, for instance, $Z=U$. Then, $X=W$; that is,

$$\langle F_{4,W}^{(+)}F_{fj,U}^{(+)}F_{fk,W}^{(+)}F_{3,U}^{(+)}\rangle = \frac{(-1)^{j+1}}{2}g^2VV'\nu^2(0)F(W,U).$$
(51)

Exchanging X and Z in **Eq. 50** and taking $U=Z$, we get

$$\langle F_{4,U}^{(+)}F_{fj,U}^{(+)}F_{fk,W}^{(+)}F_{3,W}^{(+)}\rangle = \frac{(-1)^j}{2}g^2VV'\nu^2(0)F(U,W).$$
(52)

Now, dividing **Eqs 51** and **52**, the searched result is found:

$$\frac{\langle F_{4,W}^{(+)}F_{fj,U}^{(+)}F_{fk,W}^{(+)}F_{3,U}^{(+)}\rangle}{\langle F_{4,U}^{(+)}F_{fj,U}^{(+)}F_{fk,W}^{(+)}F_{3,W}^{(+)}\rangle} = -\frac{F(W,U)}{F(U,W)}.$$
(53)

The minus sign in the above expression is independent of the concrete matrix $\widehat{P}$ representing the transformation of beam $\mathbf{F}_1^{(+)}$.

Equation 53 is only fulfilled in the cases of $U \neq W$ and $j \neq k$. In the cases of $U \neq W$ and $j = k$, there is no sign flip under the exchange $X\leftrightarrow Z$, as it can be easily demonstrated using **Eq. 43**, by putting $\tilde{F}(U,W) = 1 - \delta_{UW}$. We have the following:

$$\frac{\langle F_{4,W}^{(+)} F_{fj,U}^{(+)} F_{fj,W}^{(+)} F_{3,U}^{(+)} \rangle}{\langle F_{4,U}^{(+)} F_{fj,U}^{(+)} F_{fj,W}^{(+)} F_{3,W}^{(+)} \rangle} = \frac{F(W,U)}{F(U,W)}. \tag{54}$$

In this case, Alice must only inform Bob about her result via a classical communication channel, and Bob would modify beam $\mathbf{F}_3^{(+)}$ by applying a phase shift of p between the vertical and horizontal components of $\mathbf{F}_3^{(+)}$; that is,

$$\widehat{C} = \begin{pmatrix} 1 & 0 \\ 0 & -1 \end{pmatrix} \Rightarrow F'^{(+)}_3 = \widehat{C}\mathbf{F}_3^{(+)} = \begin{pmatrix} F'^{(+)}_q \\ F'^{(+)}_r \end{pmatrix}. \tag{55}$$

In this situation, using **Eq. 43** for $\widehat{A} = \widehat{I}$, that is, $\mathbf{F}_{3A}^{(+)} = \mathbf{F}'^{(+)}_3$, the following result was obtained:

$$\frac{\langle F_{4,W}^{(+)} F_{fj,U}^{(+)} F_{fj,W}^{(+)} F'^{(+)}_{3,U} \rangle}{\langle F_{4,U}^{(+)} F_{fj,U}^{(+)} F_{fj,W}^{(+)} F'^{(+)}_{3,W} \rangle} = -\frac{F(W,U)}{F(U,W)}. \tag{56}$$

At this point, a comment is in order. Given that Bob must wait to receive the classical information coming from Alice's station, the description of teleportation in the WRHP formalism admits a causal interpretation. Let T_{cc} be the time interval corresponding to the classical communication. If, for instance, the field amplitudes $\mathbf{F}_4^{(+)}$ and $\mathbf{F}_{fj}^{(+)}$ $(j = 1, 2)$ are defined at time t_A, then the signal at Bob's station, $F'^{(+)}_3$, must be defined at time $t_B = t_A + T_{cc}$. For simplicity, let us consider an identical path length, d_{SA}, between the source and any of the detectors TH, TV, f_{jH}, and f_{jV}. And let d_{SB} be the corresponding path length between the crystal and the position where Bob applies the transformation given in **Eq. 55**. From **Eqs 7** and **20**, the following condition must be fulfilled to achieve the teleportation protocol [33]:

$$\left| T_{cc} + \frac{d_{SA} - d_{SB}}{c} \right| \le \tau. \tag{57}$$

4 ZERO-POINT FIELD INPUTS AND BELL STATE MEASUREMENT IN THE INNSBRUCK EXPERIMENT

The role of the ZPF inputs in Bell state analysis has been investigated in previous works [31, 33, 34] by focusing on Bell state distinguishability of two photons, entangled in n dichotomic degrees of freedom, which are not mixed at the analyzer, and BSM of the one-photon polarization-momentum Bell states. The common denominator is the relationship between distinguishability of Bell states and an adequate balance between the number of amplified sets of ZPF modes entering the analyzer and the number of the sets of ZPF modes entering the idle channels located inside the analyzer.

The situation described in **Figure 1** is more involved. The information concerning the two couples of downconverted photos is carried out by the eight sets of ZPF modes entering the crystal. Two uncorrelated beams, $\mathbf{F}_{1P}^{(+)}$ and $\mathbf{F}_2^{(+)}$, are brought together at the beam splitter for Bell state analysis. Although this

situation needs further consideration, the impossibility of measuring the four polarization Bell states will be addressed on the basis of the arguments set out below.

Let us analyze the interference of beams $\mathbf{F}_{1P}^{(+)}$ and $\mathbf{F}_2^{(+)}$ at the beam splitter (see **Eqs 18** and **26**) to give the exiting fields $\mathbf{F}_{f1}^{(+)}$ and $\mathbf{F}_{f2}^{(+)}$ shown in **Eq. 33**. The intensity corresponding to $\mathbf{F}_{fj}^{(+)}$ $(j = 1, 2)$ is

$$I_j = \mathbf{F}_{fj}^{(+)} \cdot \mathbf{F}_{fj}^{(-)} = I_{H,j} + I_{V,j}, \tag{58}$$

where $I_{X,j}$ $(X = \{H, V\})$ is the intensity corresponding to the polarization component X. By putting $F_{1P,X}^{(+)} = \left| F_{1P,X}^{(+)} \right| \exp(i\varphi_{1P,X})$ and $F_{2,X}^{(+)} = \left| F_{2,X}^{(+)} \right| \exp(i\varphi_{2,X})$, it is immediate that

$$I_{X,j} = \frac{1}{2} \left[\left| F_{1P,X}^{(+)} \right|^2 + \left| F_{2,X}^{(+)} \right|^2 + 2(-1)^{j+1} \left| F_{1P,X}^{(+)} \right| \left| F_{2,X}^{(+)} \right| \sin\left(\varphi_{2,X} - \varphi_{1P,X} \right) \right], \tag{59}$$

where $I_{X,1}$ and $I_{X,2}$ contain an identical contribution, $(\left| F_{1P,X}^{(+)} \right|^2 + \left| F_{2,X}^{(+)} \right|^2)/2$, along with an addend that represents the interference between $F_{1P,X}^{(+)}$ and $F_{2,X}^{(+)}$, with opposite values for $I_{X,1}$ and $I_{X,2}$. This result is similar to the anticorrelation after a beam splitter described in stochastic optics [28], the only difference being that, in this case, both input channels contain one photon.

By taking into consideration the zero-point beam entering PBSfj and **Eqs 34** and **35**, the intensity at the detector $f_{j,X}$ is

$$I_{fj,X} = I_{X,j} + \left| F_{ZPFfj,Y}^{(+)} \right|^2; Y \ne X. \tag{60}$$

Given that detection implies noise subtraction (see **Eq. 8**), the intensity above the zero-point background is

$$I_{fj,X} - \left(I_{fj,X} \right)_{vac} = I_{X,j} - \left(I_{X,j} \right)_{vac}, \tag{61}$$

so that the zero-point contribution coming from $\mathbf{F}_{ZPFfj}$ and the pure zero-point contribution coming from the beams entering Alice's station are subtracted.

At this point, the following conjecture is applied: for an ideal detector f_{jX} $(K_{fjX} = 1)$, a detection is produced when a constructive interference between $F_{1P,X}^{(+)}$ and $F_{2,X}^{(+)}$ is produced; that is, $(-1)^{j+1} \sin(\varphi_{2,X} - \varphi_{1P,X}) = 1$, which necessarily implies a destructive interference at detector $f_{k,X}$ $(k \ne j)$. For this reason, a joint detection in detectors $f_{1,H}$ $(f_{1,V})$ and $f_{2,H}$ $(f_{2,V})$ cannot be produced. In terms of the quadruple correlations properties of the field, this result is explained in **Eq. 44**.

If detection is produced in, for example, $f_{1,H}$, it is revealed that $\varphi_{2,H} - \varphi_{1P,H} = \pi(1 + 4n)/2$, $n = 0, 1, 2...$. Then, the second detection event could be produced at the same detector $f_{1,H}$ or in one of the detectors $f_{1,V}$ and $f_{2,V}$. The question that arises is how many sets of ZPF modes, coming from the idle channels located inside the analyzer, must be subtracted to complete the phase information at Alice's station? The answer is as follows: as a minimum, one of the sets of ZPF modes entering $f_{1,V}$ and $f_{2,V}$, coming from the PBSs placed at Alice's station, should be subtracted, so that the different possibilities for the second detection would be identified.

The classical information that can be obtained in the measurement entails the subtraction of a sufficient number of sets of ZPF modes entering the idle channels inside the analyzer
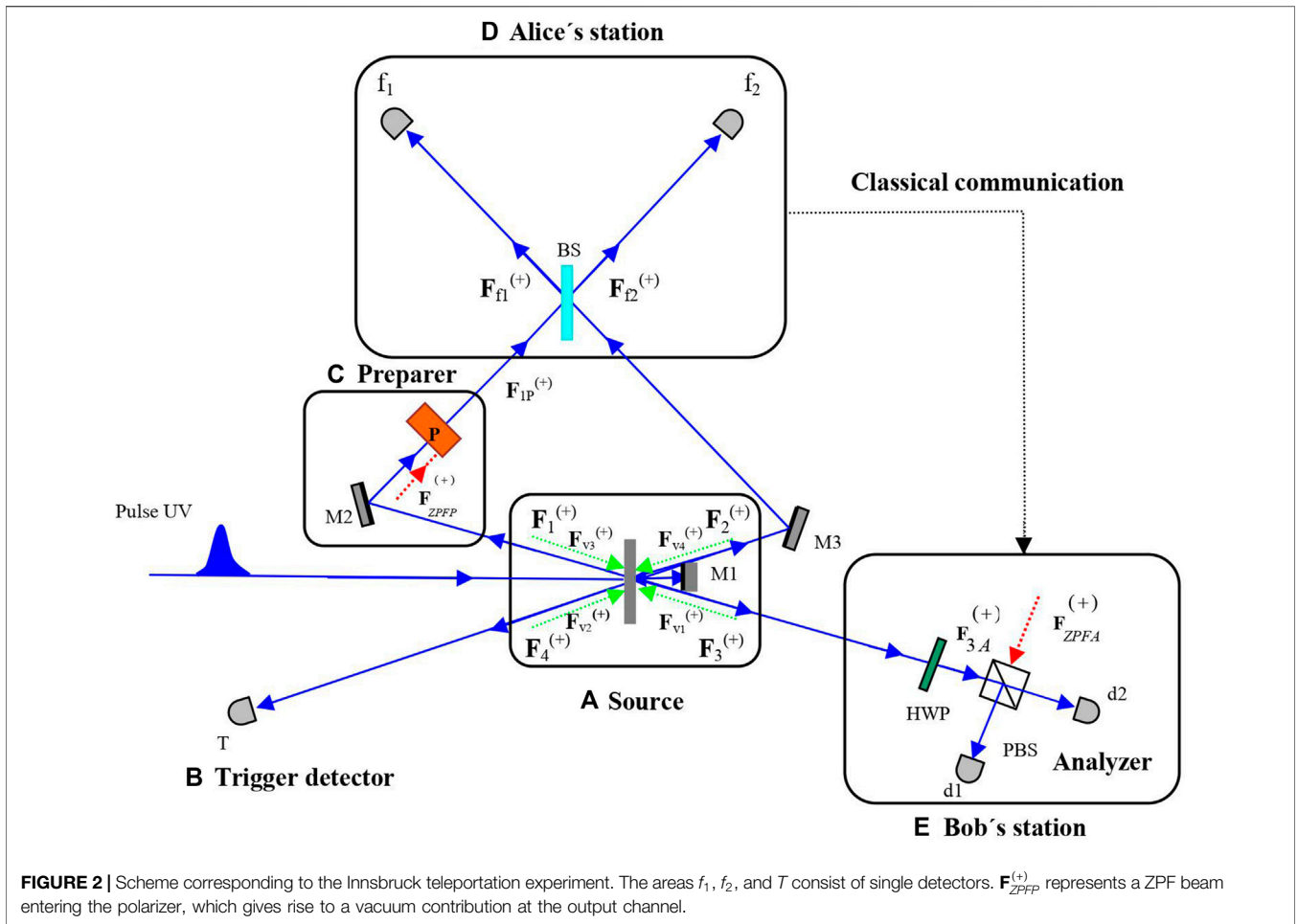
FIGURE 2 | Scheme corresponding to the Innsbruck teleportation experiment. The areas f_1, f_2, and T consist of single detectors. $\mathbf{F}_{ZPFP}^{(+)}$ represents a ZPF beam entering the polarizer, which gives rise to a vacuum contribution at the output channel.

from the number of amplified sets of modes that enter the analyzer (see **Eq. 32**). Hence, the difference $4 - 1 = 3$ gives the maximum distinguishability, which corresponds to the experimental situation.

5 FOURFOLD COINCIDENCES IN THE INNSBRUCK EXPERIMENT

Let us consider the experimental arrangement in **Figure 2** [5]. The signal $\mathbf{F}_1^{(+)}$ is sent to a polarizer P of angle $\theta = 45°$ ($\theta = -45°$) with respect to horizontal. The corresponding expression for $\mathbf{F}_{1P}^{(+)}$ is given by **Eqs 27** and **28**, where $L_H = R_V = 1/2$ and $R_H = L_V = 1/2$ ($-1/2$). In this situation, **Eq. 30** leads to $F(U, W) = F(W, U)$, so that (see **Eq. 53**)

$$\langle F_{4,W}^{(+)} F_{fj,U}^{(+)} F_{fk,W}^{(+)} F_{3,U}^{(+)} \rangle = -\langle F_{4,U}^{(+)} F_{fj,U}^{(+)} F_{fk,W}^{(+)} F_{3,W}^{(+)} \rangle. \tag{62}$$

The polarization analyzer consists of a half-wave plate (HWP) that rotates the polarization plane of $\mathbf{F}_3^{(+)}$ by an angle of $45°$ around the propagation direction and a PBS that transmits (reflects) horizontal (vertical) polarization. The field amplitudes at the detectors $d1$ and $d2$ are given by **Eq. 39**,

where $\tilde{A}_H$ and $\tilde{A}_V$ are given by **Eqs 37** and **38**, respectively, with $\tilde{L}_H = \tilde{R}_H = \tilde{L}_V = 1/\sqrt{2}$ and $\tilde{R}_V = -1/\sqrt{2}$. In this particular setting, a fourfold detection in T, f_1, f_2, and $d2$ ($d1$) is produced for $\theta = 45°$ ($\theta = -45°$).

The quadruple correlations can be calculated by using **Eq. 43**. We get the following:

Case I ($\theta = +45°$).

$$\langle F_{4,V}^{(+)} F_{fj,H}^{(+)} F_{fk,V}^{(+)} F_{3A,H}^{(+)} \rangle = \frac{g^2 VV' \nu^2(0)}{2\sqrt{2}} (-1)^j, \tag{63}$$

$$\langle F_{4,H}^{(+)} F_{fj,H}^{(+)} F_{fk,V}^{(+)} F_{3A,H}^{(+)} \rangle = \frac{g^2 VV' \nu^2(0)}{2\sqrt{2}} i(-1)^j, \tag{64}$$

$$\langle F_{4,V}^{(+)} F_{fj,H}^{(+)} F_{fk,V}^{(+)} F_{3A,V}^{(+)} \rangle = \langle F_{4,H}^{(+)} F_{fj,H}^{(+)} F_{fk,V}^{(+)} F_{3A,V}^{(+)} \rangle = 0. \tag{65}$$

Case II ($\theta = -45°$).

$$\langle F_{4,H}^{(+)} F_{fj,H}^{(+)} F_{fk,V}^{(+)} F_{3A,V}^{(+)} \rangle = \frac{g^2 VV' \nu^2(0)}{2\sqrt{2}} (-1)^j, \tag{66}$$

$$\langle F_{4,V}^{(+)} F_{fj,H}^{(+)} F_{fk,V}^{(+)} F_{3A,V}^{(+)} \rangle = \frac{g^2 VV' \nu^2(0)}{2\sqrt{2}} i(-1)^j, \tag{67}$$

$$\langle F_{4,H}^{(+)} F_{fj,H}^{(+)} F_{fk,V}^{(+)} F_{3A,H}^{(+)} \rangle = \langle F_{4,V}^{(+)} F_{fj,H}^{(+)} F_{fk,V}^{(+)} F_{3A,H}^{(+)} \rangle = 0. \tag{68}$$

A quick look at **Eqs 63–65** shows that only the two correlations involving the horizontal component of $\mathbf{F}_{3A}^{(+)}$ are different from zero. This situation reveals the teleportation of the polarization properties of beam $\mathbf{F}_{1P}$ (polarized at +45°) to $F_{3A,H}$ (detection in $d2$). Similarly, the teleportation from $\mathbf{F}_{1P}^{(+)}$ (polarized at −45°) to $F_{3A,V}^{(+)}$ can be inferred from **Eqs 66–68**.

To obtain the fourfold detection probabilities in the WRHP formalism, **Eq. 10** must be used, with $a \equiv T$, $b \equiv f_1$, $c \equiv f_2$, and $d = d_i (i = 1, 2)$. Each summation has sixteen addends. Given that the vacuum contribution at $d_i (i = 1, 2)$ coming from $\mathbf{F}_{ZPFA}^{(+)}$ is uncorrelated with the other signals and the quadruple correlations involving the same polarization at detectors f_1 and f_2 are zero (see **Eq. 44**), the sum is reduced to four addends. By using **Eqs 63–68**, the corresponding detection probabilities are as follows:

- For $\theta = 45°$,

$$P_{T,f1,f2,d1} = 0, \tag{69}$$

$$\frac{P_{T,f1,f2,d2}}{K_T K_{f1} K_{f2} K_{d2}} = \frac{g^4 |V|^4 |\nu(0)|^4}{8}. \tag{70}$$

- For $\theta = -45°$,

$$\frac{P_{T,f1,f2,d1}}{K_T K_{f1} K_{f2} K_{d1}} = \frac{g^4 |V|^4 |\nu(0)|^4}{8}, \tag{71}$$

$$P_{T,f1,f2,d2} = 0. \tag{72}$$

6 DISCUSSION AND CONCLUSION

In this article, it has been shown that the quintessential experiment on quantum teleportation, the Innsbruck experiment, can be understood without the consideration of collapse and entanglement as necessary ingredients. Compared to the classical theoretical treatment of this experiment, the consideration of the ZPF as a real field adds new physical insights that were not previously discovered. First of all, the quantum information is carried out by eight sets of ZPF modes entering the crystal, so that the physical meaning of entanglement can be found in the correlations that characterize vacuum amplitudes distributed in the emitted signals. Second, the projection postulate is closely related to the subtraction of the zero-point intensity at the detectors, in such a way that the vacuum inputs located at the idle channels inside the analyzer limit the distinguishability at Alice's station. In this sense, the WRHP formalism provides a more complete description than the one provided by the standard particle-like image in terms of photons. This is in consonance with recent approaches to the quantum jumps, where a deeper insight into the projection postulate is obtained [36].

In the WRHP approach, the teleportation of the prepared state once the trigger detector fires, under the condition of a joint detection in areas $f1$ and $f2$, is discovered by means of the quadruple correlation properties of the field and its propagation throughout the setup. The antisymmetry requirements, fulfilled in **Eqs 49** and **62**, constitute the mathematical properties leading to teleportation in the Innsbruck experiment [5]. In a general transformation represented by the matrix $\hat{P}$, teleportation is explained based on **Eqs 49** and **53**. Moreover, **Eq. 53** is required for understanding the possibility of reproducing the prepared state, in the case of a joint detection at separated detectors in areas $f1$ or $f2$ (see **Eq. 56**). In this sense, the consideration of the classical communication time in the quadruple correlation (see **Eq. 57**) reinforces the idea of a causal interpretation of teleportation.

The role of the zero-point intensity as a threshold for detection has been applied elsewhere to Bell state analysis [31, 33, 34]. In this article, new advances have been made in this area. The maximum Bell state distinguishability of two photons that are mixed at a beam splitter has been treated in this work for the first time, in the special situation of two uncorrelated beams entering the analyzer, of the four two-by-two correlated photons emitted by the source in the Innsbruck experiment. The possibility of measuring only three classes of the four polarization Bell states is based on the subtraction between the four sets of amplified modes entering the analyzer and one of the four sets of ZPF modes that enter the idle channels inside Alice's station. The role of the phases of the signals entering the analyzer as hidden variables and the consideration of the ZPF entering the vacuum channels of the PBSs as a source of noise that limits the capacity for distinguishing Bell states provide new insights that require further consideration.

At this point, some comments are in order. The statement that the information about teleportation is carried out by field amplitudes and supported by the quadruple correlations sharply contrasts with the standard description in the Hilbert space. The collapse of the four-photon state mediated by detection at the trigger detection area leads to a three-particle state (see **Eq. 12**) that constitutes the starting point of the teleportation protocol [11]. The projection of this vector via BSM at Alice's station results in a nonlocal change of the physical properties of light at Bob's side, which is identified throughout the classical communication between Alice and Bob. This conundrum of the quantum theory, which conjugates nonlocality and the superposition principle, can be solved using the WRHP formalism. On the one hand, the odd-order correlations are identically zero for Gaussian processes, so that no information about teleportation can be extracted by looking at the "triple" correlation properties of the fields $\mathbf{F}_{1P}^{(+)}$, $\mathbf{F}_2^{(+)}$, and $\mathbf{F}_3^{(+)}$. Furthermore, the Wigner distribution of the four-photon state is positive, so that a picture in terms of stochastic processes is plausible. In contrast, the corresponding one to the state given in **Eq. 12** is not positive-definite. In this sense, we emphasize that the physical properties of photon 1 are inherently linked to photon 4 through the cross-correlation properties of the light field. Hence, the consideration of the prepared state as a single-photon state is an oversimplification that hides the essential nature of teleportation, that is, the possibility of transferring the physical properties from one location to another, mediated by the zero-point fluctuations of the electromagnetic field.

The WRHP formalism bridges the gap between quantum optics and stochastic optics [37] by considering the vacuum field as a real stochastic field. Moreover, one of the main advantages of using this approach is the possibility of investigating the role of ZPF amplitudes as hidden variables to obtain information regarding the internal mechanism leading to teleportation. This analysis will be further developed in future studies.

DATA AVAILABILITY STATEMENT

The original contributions presented in the study are included in the article/Supplementary Material; further inquiries can be directed to the corresponding author.

REFERENCES

1. Bennett CH, Brassard G, Crépeau C, Jozsa R, Peres A, Wootters WK. Teleporting an unknown quantum state via dual classical and Einstein-Podolsky-Rosen channels. *Phys Rev Lett* (1993) 70:1895–9. doi:10.1103/PhysRevLett.70.1895

2. Llewellyn DM, Ding Y, Faruque II, Paesani S, Bacco D, Santagati R, et al. Chip-to-chip quantum teleportation and multi-photon entanglement in silicon. *Nat Phys* (2020) 16:148–53. doi:10.1038/s41567-019-0727-x

3. Luo Y-H, Zhong H-S, Erhard M, Wang X-L, Peng L-C, Krenn M, et al. Quantum Teleportation in high dimensions. *Phys Rev Lett* (2019) 123: 070505. doi:10.1103/PhysRevLett.123.070505

4. Einstein A, Podolsky B, Rosen N. Can quantum-mechanical description of physical reality be considered complete? *Phys Rev* (1935) 47:777. doi:10.1103/PhysRev.47.777

5. Bouwmeester D, Pan J-W, Mattle K, Eibl M, Weinfurter H, Zeilinger A. Experimental quantum teleportation. *Nature* (1997) 390:575–9. doi:10.1038/37539

6. Boschi D, Branca S, De Martini F, Hardy L, Popescu S. Experimental realization of teleporting an unknown pure quantum state via dual classical and Einstein-Podolsky-Rosen channels. *Phys Rev Lett* (1998) 80:1121–5. doi:10.1103/PhysRevLett.80.1121

7. De Martini F. Teleportation: who was first? *Phys World* (1998) 11:23–4. doi:10.1088/2058-7058/11/3/21

8. Bouwmeester D, Pan J-W, Weinfurter H, Zeilinger A. High-fidelity teleportation of independent qubits. *J Mod Optic* (2000) 47:279–89. doi:10.1080/09500340008244042

9. Yurke B, Stoler D. Einstein-Podolsky-Rosen effects from independent particle sources. *Phys Rev Lett* (1992) 68:1251–4. doi:10.1103/PhysRevLett.68.1251

10. Pan J-W, Bouwmeester D, Weinfurter H, Zeilinger A. Experimental entanglement swapping: entangling photons that never interacted. *Phys Rev Lett* (1998) 80:3891. doi:10.1103/PhysRevLett.80.3891

11. Mattle K, Weinfurter H, Kwait PG, Zeilinger A. Dense coding in experimental quantum communication. *Phys Rev Lett* (1996) 76:4656–9. doi:10.1103/PhysRevLett.76.4656

12. Braunstein SL, Kimble HJ. A posterior teleportation. *Nature* (1998) 394: 840–41. doi:10.1038/29674

13. Bouwmeester D, Pan J-W, Daniell M, Weinfurter H, Zukowski M, Zeilinger A. Reply: a posterior teleportation. *Nature* (1998) 394:841. doi:10.1038/29678

14. Kok P, Braunstein SL. Postselected versus nonpostselected quantum teleportation using parametric down-conversion. *Phys Rev* (2000) 61: 042304. doi:10.1103/PhysRevA.61.042304

15. Popescu S. An optical method for teleportation (1995) arxiv:9501020.

16. Michler M, Risco-Delgado R, Weinfurter H. Remote state preparation. *Technical. Digest. EQEC* (1998) 1:99. doi:10.1109/EQEC.1998.714868

AUTHOR CONTRIBUTIONS

AC has conducted the whole research in the article, the organization of the manuscript, calculations, and the main ideas in the text. SG has contributed to the calculations, figures, and text elaboration, along with useful discussions concerning the essential ideas. JP has contributed to the discussions of the main ideas related to this research.

ACKNOWLEDGMENTS

17. Casado A, Marshall TW, Santos E. Parametric downconversion experiments in the Wigner representation. *J Opt Soc Am B* (1997) 14:494–502. doi:10.1364/JOSAB.14.000494

18. Casado A, Fernández-Rueda A, Marshall TW, Risco-Delgado R, Santos E. Fourth-order interference in the Wigner representation for parametric down-conversion experiments. *Phys Rev* (1997) 55:3879–90. doi:10.1103/PhysRevA.55.3879

19. Casado A, Marshall TW, Santos E. Type-II parametric downconversion in the Wigner function formalism: entanglement and Bell's inequalities. *J Opt Soc Am B* (1998) 15:1572–7. doi:10.1364/JOSAB.15.001572

20. Casado A, Fernández-Rueda A, Marshall TW, Risco-Delgado R, Santos E. Dispersion cancellation and quantum eraser experiments analyzed in the Wigner function formalism. *Phys Rev* (1997) 56:2477–80. doi:10.1103/PhysRevA.56.2477

21. Casado A, Fernández-Rueda A, Marshall TW, Martínez J, Risco-Delgado R, Santos E. Dependence on crystal parameters of the correlation time between signal and idler beams in parametric down conversion calculated in the Wigner representation. *Eur Phys J D* (2000) 11:465–72. doi:10.1007/s100530070074

22. Casado A, Marshall TW, Risco-Delgado R. Spectrum of the parametric down converted radiation calculated in the Wigner function formalism. *Eur Phys J D* (2001) 13:109–19. doi:10.1007/s100530170292

23. Dechoum K, Marshall TW, Santos E. Parametric down and up conversion in the Wigner representation of quantum optics. *J Mod Optic* (2000) 47:1273–87. doi:10.1080/095003400147575

24. Casado A, Risco-Delgado R, Santos E. Local realistic theory for PDC experiments based on the Wigner formalism. *Z Naturforsch* (2001) 56A: 178–81. doi:10.1515/zna-2001-0129

25. Casado A, Marshall TW, Risco-Delgado R, Santos E. A Local hidden variables model for experiments involving photon pairs produced in parametric down conversion (2002) arXiv:quant-ph/0202097v1.

26. Santos E. Local realistic interpretation of entangled photon pairs in the Weyl-Wigner formalism (2020) arXiv:1908.03924v4 [quant-ph].

27. Santos E. Can quantum vacuum fluctuations be considered real? (2002) arxiv: 0206161.

28. Santos E. Photons are fluctuations of a random (zeropoint) radiation filling the whole space. *Proc SPIE* (2005) 5866:36–7. doi:10.1117/12.619611

29. Casado A, Guerra S, Plácido J. Wigner representation for experiments on quantum cryptography using two-photon polarization entanglement produced in parametric down-conversion. *J Phys B Atom Mol Opt Phys* (2008) 41:045501. doi:10.1088/0953-4075/41/4/045501

30. Casado A, Guerra S, Plácido J. Partial Bell-state analysis with parametric down conversion in the Wigner function formalism. *J Adv Math Phys* (2010) 2010: 501521. doi:10.1155/2010/501521

31. Casado A, Guerra S, Plácido J. Wigner representation for polarization-momentum hyperentanglement generated in parametric down-conversion,

and its application to complete Bell-state measurement. *Eur Phys J D* (2014) 68:
338. doi:10.1140/epjd/e2014-50368-y

32. Casado A, Guerra S, Plácido J. Wigner representation for entanglement
swapping using parametric down conversion: the role of vacuum
fluctuations in teleportation. *J Mod Optic* (2015) 62:377–86. doi:10.1080/
09500340.2014.983571

33. Casado A, Guerra S, Plácido J. Rome teleportation experiment
analysed in the Wigner representation: the role of the zeropoint
fluctuations in complete one-photon polarization-momentum Bell-
state analysis. *J Mod Optic* (2018) 65:1960–74. doi:10.1080/
09500340.2018.1478009

34. Casado A, Guerra S, Plácido J. From stochastic optics to the Wigner formalism:
the role of the vacuum field in optical quantum communication experiments.
Atoms (2019) 7:76. doi:10.3390/atoms7030076

35. Clauser JF, Horne M. Experimental consequences of objective local theories.
Phys Rev D. (1974) 10:526–35. doi:10.1103/PhysRevD.10.526

36. Minev ZK, Mundhada SO, Shankar S, Reinhold P, Gutiérrez-Jáuregui R,
Schoelkopf RJ, et al. To catch and reverse a quantum jump mid-flight.
Nature (2019) 570:200–204. doi:10.1038/s41586-019-1287-z

37. Marshall TW, Santos E. Stochastic optics: a reaffirmation of the wave nature of
light. *Found Phys* (1988) 18:185–223. doi:10.1007/BF01882931